

mvHOTA: A multi-view higher order tracking accuracy metric to measure spatial and temporal associations in multi-point detection

Lalith Sharan^{1,2}[000–0003–0835–042X], Halvar Kelm¹, Gabriele Romano³,
Matthias Karck³, Raffaele De Simone³, and Sandy
Engelhardt^{1,2}[0000–0001–8816–7654]

¹ Department of Internal Medicine III, Heidelberg University Hospital, Heidelberg

² DZHK (German Centre for Cardiovascular Research), partner site
Heidelberg/Mannheim

³ Department of Cardiac Surgery, Heidelberg University Hospital, Heidelberg

Abstract. Multi-object tracking (MOT) is a challenging task that involves detecting objects in the scene and tracking them across a sequence of frames. Evaluating this task is difficult due to temporal occlusions, and varying trajectories across a sequence of images. The main evaluation metric to benchmark MOT methods on datasets such as KITTI has recently become the *higher order tracking accuracy* (HOTA) metric, which is capable of providing a better description of the performance over metrics such as MOTA, DetA, and IDF1. Point detection and tracking is a closely related task, which could be regarded as a special case of object detection. However, there are differences in evaluating the detection task itself (point distances vs. bounding box overlap). When including the temporal dimension and multi-view scenarios, the evaluation task becomes even more complex. In this work, we propose a multi-view higher order tracking metric (mvHOTA) to determine the accuracy of multi-point (multi-instance and multi-class) detection, while taking into account temporal and spatial associations. mvHOTA can be interpreted as the geometric mean of the detection, association, and correspondence accuracies, thereby providing equal weighting to each of the factors. We demonstrate a use-case through a publicly available endoscopic point detection dataset from a previously organised medical challenge. Furthermore, we compare with other adjusted MOT metrics for this use-case, discuss the properties of mvHOTA, and show how the proposed correspondence accuracy and the *Occlusion index* facilitate analysis of methods with respect to handling of occlusions. The code will be made publicly available.

Keywords: Evaluation metrics · Point detection · Tracking · Multi-View

1 Introduction

A range of use cases exist for point or landmark detection in the computer vision and biomedical domain. These range from motion tracking in traffic scenes [7],

pose estimation [3], and multi-view reconstruction [16]; to respiratory motion estimation [18], and surgical suture detection [17] in endoscopy. In applications where several points should be identified, they can either represent multiple instances of the same class (e.g., the same type of cell), or represent multiple classes (e.g., the tip of different surgical instruments). Similar to multi-object tracking (MOT), we refer to both cases as a *multi-point tracking* problem. Furthermore, one can differentiate between single- and multi-view settings, where the same scene or object is captured from different angles. This is typically the case in stereo-endoscopy, where correspondences need to be matched between multiple views. Here, the same point can be contained in all perspectives or might be occluded in some. In reality a point may be occluded from one frame to another, may move out of the scene and reappear, or be visible in only one of the views. This poses challenges to the proper evaluation of all involved subtasks of finding temporal associations and spatial correspondences *and* detection of the points themselves. Hence, developing a single metric which treats all of these subtasks as equally important is crucial.

Recent work in our field by the MICCAI Special Interest Group *Biomedical Image Analysis Challenges* (SIG-BIAC) [13,12] has emphasized the considerable impact of evaluation metrics in benchmarking and ranking the performance of different methods, and interpreting the results with respect to different performance criteria. Our aim is to propose an extension to current metrics in the application area of point detection, taking also into account temporal associations and/or spatial correspondences.

Although multi-point tracking is a closely related task to, and can be considered a special case of a multi-object tracking task [7,5], crucial differences exist in evaluating the intrinsic detection task. In MOT, bounding boxes are predicted for each object, where an *Intersection over Union* (IoU) is typically used to compute the overlap of a source and target bounding box (see Fig. 1(I) (a)). The IoU has the value 0 when there is no overlap, and 1 when there is complete overlap. Then, a matching algorithm is employed to match the ground-truth labels and predictions. The matches obtained through this algorithm are then filtered with

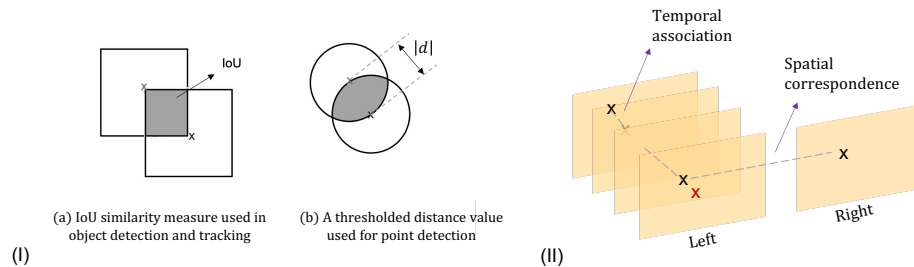


Fig. 1. (I) A sample case that shows the detection, association and correspondence (II) (a) The IoU metric used in object detection vs. (b) thresholded radius used in point detection.

a threshold α , where the label-prediction pairs with an overlap greater than α are considered a successful match. The algorithm maximises the global similarity and the number of true positive detections [11]. In contrast in point detection, the minimum distance between two points is 0, but the maximum distance is theoretically unbounded. Practically, the maximum distance between two points in an image is bounded by the image diagonal, e.g., as shown in [8]. Moreover, unlike bounding boxes, comparison in the case of point detection is equivalent to considering a radius centered around the point (see Fig. 1(I) (b)).

The previously proposed *Higher Order Tracking Accuracy* (HOTA) metric [11] equally weights the detection and temporal association, and is used by the KITTI [7] and MOT [5] benchmarks to evaluate submitted methods. In this work, we extend the HOTA metric [11] and propose a metric to evaluate the multi-view higher order tracking accuracy (*mvHOTA*) by incorporating both temporal and spatial associations (see Fig. 1(II)). This is realized by computing a *Correspondence Accuracy* (*CorresAcc*) along with detection and association accuracies. While previous work [11] presents a trivial extension to a multi-view setup, here we propose a metric that can be used to analyse the handling of spatial occlusions, along with the detection and temporal associations. We demonstrate the use of this metric on a publicly available surgical endoscopic dataset [6]. Furthermore, we present an analysis of the metric properties, and a comparison to other MOT metrics, which were adjusted to the point tracking use case.

2 Related Work

Currently, multiple metrics exist to evaluate a tracking task, albeit borrowed from the closely related task of multi-object tracking (MOT) [1,14,4]. The CLEAR-MOT [1] metrics were introduced as a standard to evaluate a range of tracking methods, and has been used for years as the standard to benchmark a range of MOT methods. Primarily, the *Multi Object Tracking Accuracy* (MOTA) and *Multi Object Tracking Precision* (MOTP) are used to track the association of detection over time. The *IDF1* proposed by Ristani et al. [14] is another metric initially proposed for use in multi-target multi-camera tracking systems and later also adopted for MOT evaluation. Track-mAP is commonly used in benchmarks such as Image-Net [15], and TAO [4], which requires the use of confidence scores along with the tracker predictions. The recently proposed *Higher Order Tracking Accuracy* (HOTA) introduced by Luiten et al. [11] has replaced many of the multi-object tracking benchmarks, for example in KITTI MOT [7] and the MOTS challenge [5]. Besides proposing a single unifying metric to measure detection and association, the work analyses the drawbacks of the previously used MOTA and IDF1 metrics in terms of monotonicity and error type differentiability, as explained by [10].

3 Methods

ID Assignment In multi-point tracking, each labelled (GT) and predicted (Pred) point is assigned an ID that denotes a unique identifier to each of the GTs and Preds across the temporal sequence and views. While GT IDs are assigned from the labels, Pred ID assignment is performed with algorithmic matching. The Hungarian matching algorithm [9] can be used to identify related points and assign the IDs [11]. The Hungarian algorithm [9] amounts to a minimum weight bipartite graph matching, where the bipartite sets of the graph represent the predictions of the current and previous frame. In multi-point tracking, the Euclidean distance $|d|_{p_{t-1}, p_t}$ between a point p_{t-1} from the previous time step and a point p_t is computed as the matching cost for this pair of points. To adapt the Hungarian algorithm [9] for multi-point tracking, we first perform thresholding and then upper bound the values of all the points that lie above the threshold, to a value of the image diagonal. We subsequently minimize this distance cost to match the IDs between one frame to another. By matching each point in the current frame with a global ID list, we can then assign the same ID to the Preds at similar locations across a temporal sequence even though they move in and out of the scene across time.

Detection The temporal ID assignment is a pre-cursor to the actual matching step between the GTs and the Preds. Once the IDs are assigned for each of the p_{gt} and p_{pred} in each views and each time step, we can now match the GT and Pred in each frame, again, using the Hungarian algorithm [9]. In this case, the two sets of a bipartite graph are the GT and Pred points respectively. If a point p_{pred} lies within the radius of threshold α , then it is a *True Positive* (TP) (see Eqn. 1). If more than one point lies within the radius, then the point with the closest distance $|d|$ is matched with the GT. A *False Negative* (FN) detection is a p_{gt} that is not matched with any p_{pred} , and a *False Positive* (FP) is a p_{pred} that is not matched with any p_{gt} . Typically, a balanced F_1 score (e.g., in [17]) is used to combine the TP, FP, and FN points in a single metric. However, the F_1 score is non-monotonic with respect to detections [11] and therefore, we use a *Jaccard* formulation to compute the detection accuracy, similar to [11].

$$TP(gt, pred) = \{p_{pred} : |d|_{p_{gt}, p_{pred}} < \alpha\} \quad (1)$$

Temporal Association Like in HOTA [11], in order to track the temporal association of the detected points, a *Jaccard* score between the GT and Pred trajectories is computed [11]. Practically, the normalised cost for each GT-Pred pair is accumulated across the temporal sequence of frames and incorporated into the matching cost. The association accuracy is computed as,

$$AssAcc = \frac{1}{|TP|} \sum_{c \in \{TP\}} \frac{|TPA(c)|}{|TPA(c)| + |FPA(c)| + |FNA(c)|} \quad (2)$$

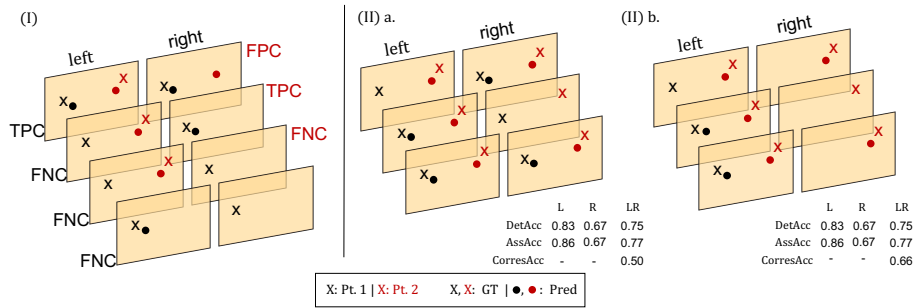


Fig. 2. (I) An illustration of the different cases of correspondence measure when GT correspondence exists (Pt. 1), and does not exist (Pt. 2) (II) An example that illustrates a change in the correspondence without a change in detection and association accuracy.

where a TPA for a point is the number of points in the sequence having the same GT and Pred IDs [11]. The points with the same GT ID but a different Pred IDs are counted as FNA, and a same Pred ID with a different GT ID is counted as a FPA. The HOTA metric combines the detection accuracy and association accuracy, to provide a balanced metric that weights both aspects equally. Additionally, the localisation accuracy can be computed as the distance cost of the points that lie within the threshold α .

Multi-view correspondence In this work, we introduce the concept of a matched correspondence between multiple views. The correspondence c_p of a point p , is defined as m , where m is the number of views where a point in a view is additionally found. For example, if a point p exists in all n views of an n camera setup, then $c_p = n - 1$. A *True Positive Correspondence* (TPC), *False Negative Correspondence* (FNC), and *False Positive Correspondence* (FPC), is computed as:

$$\forall p_{gt}, TPC : c_{pr} = c_{gt}, FPC : c_{pr} < c_{gt}, FNC : c_{pr} > c_{gt} \quad (3)$$

Fig. 2 (I) illustrates the possible scenarios for a stereo setup. For example, Pt. 1 in Fig. 2 (I) is visible in both views. Here, a TPC is defined when a TP is found in both views. An FNC is defined when there are no TP detections found for this GT in one or both the views. Pt. 2 in Fig. 2 (I), is present in only one of the views. This is a typical scenario due to occlusions or differences in field of view. Here, a TPC is defined only when a TP detection exists for the GT point in its respective view. If there are no matched TP detections, then it is an FNC, and if the Pred is found in both frames, then it is an FPC. The correspondence accuracy can then be defined as the *Jaccard* score averaged for all TP points c for each frame in the sequence, given by:

$$CorresAcc = \frac{1}{|TP|} \sum_{c \in \{TP\}} \frac{|TPC(c)|}{|TPC(c)| + |FPC(c)| + |FNC(c)} \quad (4)$$

Multi-view HOTA We now combine the above mentioned concepts of detection, association, and correspondence accuracy to formulate the multi-view higher order tracking accuracy:

$$mvHOTA = \sqrt[3]{DetAcc \cdot AssAcc \cdot CorresAcc} \quad (5)$$

Each of *AssAcc* and *CorresAcc* are averaged over each TP detection, and therefore can be seen as augmenting a TP detection score with the *AssAcc* and *CorresAcc* instead of double counting the errors. Furthermore, *mvHOTA* can be interpreted as the geometric mean of the detection, association, and correspondence accuracies, thereby providing equal weighting to each of the factors.

Occlusion Index Besides *mvHOTA*, we propose an *Occlusion index (o)*. The extent of occlusion in the dataset for an *n*-view setup, can be computed by,

$$o = 1 - \frac{|p_{corres}|}{|p_{gt}|} \quad (6)$$

where p_{corres} refers to the points that are present in all the views. Here the *Occlusion index* not only denotes the physically occluded points, but also the points that are present in only one view due to differences in camera position, or field of view. Essentially, they represent the points that do not have a correspondence.

3.1 Properties

For a single-view, single-instance tracking scenario, *mvHOTA* simplifies into a *Jaccard* formulation of $|TP|/(|TP| + |FP| + |FN|)$. Luiten et al. [11] showed that HOTA is both monotonic and differentiable into the different error types, as proposed by [10]. *mvHOTA* follows a similar formulation while including the correspondence information between the multiple views. Furthermore, the interpretation as the geometric mean ensures the metric is balanced between the different aspects of detection, tracking, and correspondence. The ability to differentiate the metric into different error types [10] and analyse their aspects is especially crucial for benchmarking, ranking, and interpreting the performance of the different methods. More information can be found in Appendix C.

4 Experiments and Results

In this section we present two application scenarios of the *mvHOTA* metric. Firstly, we construct a toy example to demonstrate how *mvHOTA* can accommodate the correspondence information from different views, when other factors are unchanged. Secondly, we present a use-case on an endoscopic dataset in surgery and show how to use this metric on a real-life dataset.

Toy dataset Fig. 2 (II) represents an example case in point detection with two GT IDs. Fig. 2 (II)a. contains two GT points and their respective predictions. In Fig. 2 (II)b., we now remove one of the GT IDs and the associated predictions. This changes the correspondence without affecting the detection and association accuracies. Here, *mvHOTA* is able to accommodate this change, while computing the MOT metrics for each view (see Tab. 1) does not account for the correspondence. A further example of *mvHOTA* applied to more than two views can be found in Appendix D.

Endoscopic dataset In this work, we demonstrate the use of the *mvHOTA* metric in a multi-point detection and tracking problem in surgery. The mitral valve dataset is an endoscopic dataset acquired from minimally invasive mitral valve repair [6,17], comprising images captured from a stereo-endoscope. Occlusions are present between the two views and in the temporal domain with respect to the points of interest, e.g. surgical instruments may occlude parts of the sutures. An illustration of this is shown in Fig. 3 where cases of temporal occlusions and cases of spatial occlusions can be seen. Additionally the *Occlusion index* (o) indicates the fraction of points that are occluded (computed for GTs for each frame in Fig. 3). The multi-point task is to detect the entry and exit points of sutures, which are stitched. The suture points do not occur at anatomically unique locations and the number of suture points vary in each image temporally and between the views. The dataset was made publicly available as part of the AdaptOR challenge [6].

Other works have primarily focused on the detection task and treated the stereo-information as two mono instances. Furthermore, they have formulated it as a multi-instance heatmap regression problem [17,19]. Evaluation was done using a balanced F_1 score. A threshold of $6px$ was set as the similarity threshold, as it roughly corresponds to the thickness of the suture in this image resolution. In this work, we additionally focus on the stereo as well as on the temporal information. We build on the detection method described in [17], and use the Hungarian matching algorithm with a thresholded distance computation to assign the IDs temporally in each view. Additionally a global GT ID list is created that includes a union of points found in both views, and a per-view contiguous list of IDs is created to be able to apply the matching algorithm. By then counting the number of matches accumulated for each ID, we can compute the detection and association metrics. In order to compute the correspondence accuracy, we compare the correspondences of the GT points before and after matching with the predictions.

Table 1. Comparison of MOT metrics on the two cases of the toy example as shown in Fig. 2 (II). Change in *mvHOTA* is highlighted in bold.

Case	MOTA	IDF1	F1	HOTA	mvHOTA
(II)a.	0.58	0.76	0.85	0.76	0.66
(II)b.	0.58	0.76	0.85	0.76	0.73

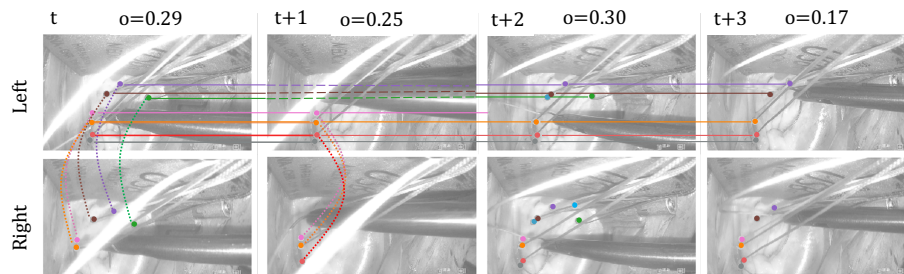


Fig. 3. An example from the stereo-endoscopic dataset that illustrates occlusions in the temporal and spatial domains. A suture is assigned a unique ID across views and time (the colors represent the IDs). A point can disappear and appear in view due to temporal (brown, left, t to $t+2$) or spatial (red, left vs. right) occlusion. For all frames in this figure, the average $o = 0.25$.

Table 2. Comparison of MOT metrics on the surgical endoscopic dataset. The MOTA, IDF1, F1, and HOTA metrics are averaged for each view.

Metric	MOTA	IDF1	F1	DetAcc	AssAcc	HOTA	CorresAcc	mvHOTA
AdaptOR	-0.059	0.127	0.328	0.219	0.202	0.205	0.206	0.207

Table 2 presents the evaluation of the suture point detection method, in comparison with various MOT metrics, which were adjusted to the multi-view point detection and tracking case. It can be seen that since the method is not optimised for point tracking, but rather for point detection, the association accuracy is low, while the $F1$ score is higher. The dataset has an *Occlusion index* (o) of 41.98%. The multi-view *DetAcc* is 21.9%, *AssAcc* 20.2%, and the *CorressAcc* 20.6%. The *CorressAcc* indicates how well the model was able to handle the presence of spatial occlusions in the dataset. In this dataset, the low scores of *AssAcc* and *CorressAcc* indicate that the model performs poorly when it comes to detecting points consistently temporally and spatially across the views.

5 Discussion and Conclusion

While a range of metrics have been proposed to evaluate a MOT task [1,4,14], in this work we propose a metric to track spatial and temporal association in multi-point tracking. Different endoscopic datasets, be it laparoscopy [2] or heart surgery [17], contain varying amounts of temporal or spatial occlusions depending on the moving or static nature of the camera and the scene. The *mvHOTA* metric is especially useful in this case, as it incorporates both spatial and temporal occlusion, and enables analysis and benchmarking of different aspects of a model performance. Alternatively, computing HOTA [11] for each view and averaging them, does not embed the correspondence information (see Fig. 2 (II)b.) However, there exist some limitations of *mvHOTA*. Firstly, the metric is

biased towards a complete correspondence in all views. Furthermore, the quality of temporal ID assignment has an impact on the computation of the association scores. Similar to the HOTA metric [11], *mvHOTA* cannot be used for online evaluation, since it requires the whole sequence of IDs to be able to compute a global associations. A future work is to show how the localisation accuracy is computed by averaging *mvHOTA* across multiple thresholds, so as to apply to other object detection tasks.

6 Supplemental Material

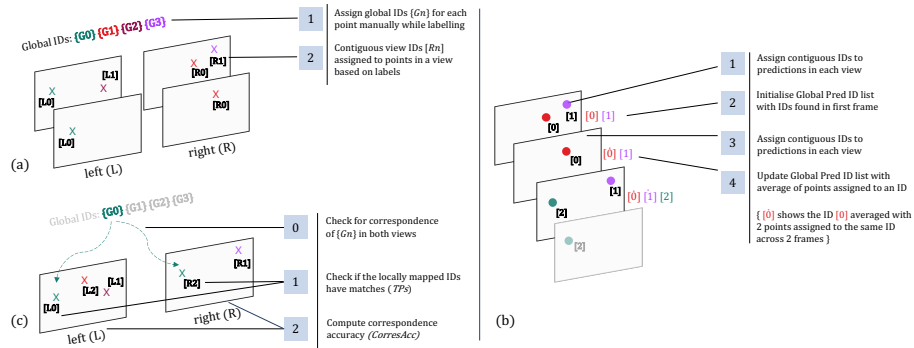


Fig. 4. Appendix A: The use of *mvHOTA* requires temporally matched IDs assigned to both the GT (x) and predicted points (●). This figure show how (a) global GT IDs are created based on labels, but are mapped to locally contiguous IDs assigned to each view. (b) Predicted points are temporally matched to a global list for each view, which is averaged after every frame is matched. (c) *CorresAcc* is computed after matching the GT with the predictions.

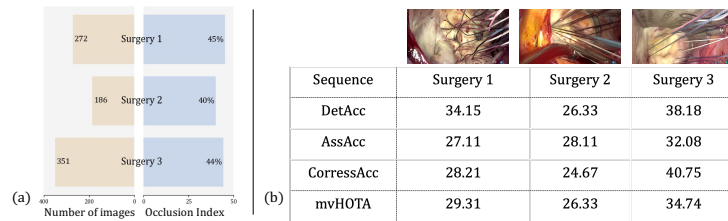


Fig. 5. Appendix B: (a) Split-up of the 3 surgeries used to compute the metrics presented for the endoscopic dataset. (b) sample images from each surgery and their respective *DetAcc*, *AssAcc*, *CorresAcc*. Surgery 1 has a lower *AssAcc* than 2, but still has a better *mvHOTA* score due to better *DetAcc* and *CorresAcc*.

Appendix C: Metric properties Evaluating a metric with respect to different aspects of performance not only helps in comparing methods, but also in aligning this comparison towards an application that favours specific aspects of performance. In this regard, [10] define 5 basic error types for MOT tasks, namely *False Negatives*, *False Positives*, *Fragmentation*, *Mergers*, and *Deviations*. [11] showed how for the tracking task HOTA decomposes into the five error types with an equivalent computation of detection recall, detection precision, association recall, association precision, and localisation. *mvHOTA* that is built upon this work can be similarly analysed with respect to the basic error types. In addition, we propose a new basic error type in a multi-view scenario, namely *Occlusions*.

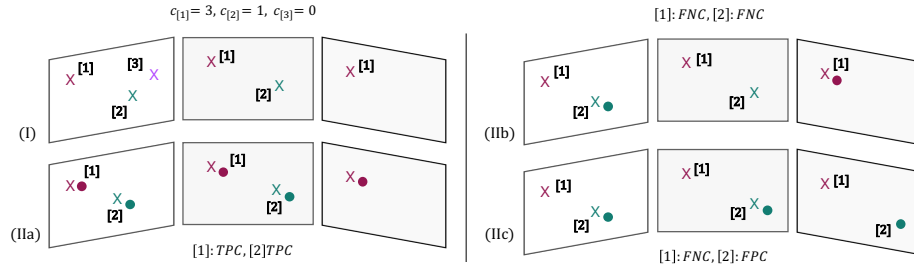


Fig. 6. Appendix D: An example illustration of a 3-view setup with GT (x) and Preds (•). (I) shows how the correspondence is calculated for each point in different scenarios. (IIa), (IIb), and (IIc) show the calculation of TPC, FPC, and FNC in each case, which is then used to compute the *CorresAcc* with a *Jaccard* formulation.

Acknowledgements This work was supported in part by Informatics for Life funded by the Klaus Tschira Foundation and the German Research Foundation DFG Project 398787259, DE 2131/2-1 and EN 1197/2-1.).

References

1. Bernardin, K., Stiefelhagen, R.: Evaluating Multiple Object Tracking Performance: The CLEAR MOT Metrics. *EURASIP Journal on Image and Video Processing* **2008**(1), 1–10 (Dec 2008). <https://doi.org/10.1155/2008/246309>
2. Bodenstedt, S., Allan, M., Agustinos, A., Du, X., Garcia-Peraza-Herrera, L., Kengott, H., Kurmann, T., Müller-Stich, B., Ourselin, S., Pakhomov, D., Sznitman, R., Teichmann, M., Thoma, M., Vercauteren, T., Voros, S., Wagner, M., Wochner, P., Maier-Hein, L., Stoyanov, D., Speidel, S.: Comparative evaluation of instrument segmentation and tracking methods in minimally invasive surgery. arXiv:1805.02475 [cs] (May 2018), <http://arxiv.org/abs/1805.02475>, arXiv:1805.02475

3. Cao, Z., Hidalgo, G., Simon, T., Wei, S.E., Sheikh, Y.: Openpose: Realtime multi-person 2d pose estimation using part affinity fields (2019)
4. Dave, A., Khurana, T., Tokmakov, P., Schmid, C., Ramanan, D.: TAO: A Large-Scale Benchmark for Tracking Any Object. In: Vedaldi, A., Bischof, H., Brox, T., Frahm, J.M. (eds.) *Computer Vision – ECCV 2020*, vol. 12350, pp. 436–454. Springer International Publishing, Cham (2020). https://doi.org/10.1007/978-3-030-58558-7_26, series Title: Lecture Notes in Computer Science
5. Dendorfer, P., Rezatofighi, H., Milan, A., Shi, J., Cremers, D., Reid, I., Roth, S., Schindler, K., Leal-Taixe, L.: CVPR19 Tracking and Detection Challenge: How crowded can it get? arXiv:1906.04567 [cs] (Jun 2019), <http://arxiv.org/abs/1906.04567>, arXiv: 1906.04567
6. Engelhardt, S., Mukhopadhyay, A., Simone, R.D., Sharan, L., Stern, A., Brand, J., Krumb, H.: Deep Generative Model Challenge for Domain Adaptation in Surgery 2021 (Mar 2021). <https://doi.org/10.5281/zenodo.4646979>, <https://zenodo.org/record/4646979>, publisher: Zenodo
7. Geiger, A., Lenz, P., Urtasun, R.: Are we ready for autonomous driving? the kitti vision benchmark suite. In: *Conference on Computer Vision and Pattern Recognition (CVPR)* (2012)
8. Koehler, S., Sharan, L., Kuhm, J., Ghanaat, A., Gordejewa, J., Simon, N.K., Grell, N.M., André, F., Engelhardt, S.: Comparison of Evaluation Metrics for Landmark Detection in CMR Images. arXiv:2201.10410 [cs] (Jan 2022), <http://arxiv.org/abs/2201.10410>, arXiv: 2201.10410
9. Kuhn, H.W.: The Hungarian method for the assignment problem. *Naval Research Logistics Quarterly* **2**(1-2), 83–97 (1955). <https://doi.org/10.1002/nav.3800020109>, <https://onlinelibrary.wiley.com/doi/abs/10.1002/nav.3800020109>, [_eprint: https://onlinelibrary.wiley.com/doi/pdf/10.1002/nav.3800020109](https://onlinelibrary.wiley.com/doi/pdf/10.1002/nav.3800020109)
10. Leichter, I., Krupka, E.: Monotonicity and error type differentiability in performance measures for target detection and tracking in video. In: *2012 IEEE Conference on Computer Vision and Pattern Recognition*. pp. 2003–2009 (Jun 2012). <https://doi.org/10.1109/CVPR.2012.6247903>, iISSN: 1063-6919
11. Luiten, J., Osep, A., Dendorfer, P., Torr, P., Geiger, A., Leal-Taixe, L., Leibe, B.: HOTA: A Higher Order Metric for Evaluating Multi-Object Tracking. *International Journal of Computer Vision* **129**(2), 548–578 (Feb 2021). <https://doi.org/10.1007/s11263-020-01375-2>, <http://arxiv.org/abs/2009.07736>, arXiv: 2009.07736
12. Maier-Hein, L., Eisenmann, M., Reinke, A., Onogur, S., Stankovic, M., Scholz, P., Arbel, T., Bogunovic, H., Bradley, A.P., Carass, A., Feldmann, C., Frangi, A.F., Full, P.M., van Ginneken, B., Hanbury, A., Honauer, K., Kozubek, M., Landman, B.A., März, K., Maier, O., Maier-Hein, K., Menze, B.H., Müller, H., Neher, P.F., Niessen, W., Rajpoot, N., Sharp, G.C., Sirinukunwattana, K., Speidel, S., Stock, C., Stoyanov, D., Taha, A.A., van der Sommen, F., Wang, C.W., Weber, M.A., Zheng, G., Jannin, P., Kopp-Schneider, A.: Why rankings of biomedical image analysis competitions should be interpreted with care. *Nature Communications* **9**(1), 5217 (Dec 2018). <https://doi.org/10.1038/s41467-018-07619-7>, <http://www.nature.com/articles/s41467-018-07619-7>
13. Reinke, A., Eisenmann, M., Tizabi, M., Sudre, C., Radsch, T., Antonelli, M., Arbel, T., Bakas, S., Cardoso, M., Cheplygina, V., Farahani, K., Glocker, B., Heckmann-Notzel, D., Isensee, F., Jannin, P., Kahn, C.E., Kleesiek, J., Kurç, T., Kozubek, M., Landman, B., Litjens, G., Maier-Hein, K.H., Menze, B., Muller, H., Petersen,

- J., Reyes, M., Rieke, N., Stieltjes, B., Summers, R., Tsaftaris, S., Ginneken, B., Kopp-Schneider, A., Jager, P.F., Maier-Hein, L.: Common Limitations of Image Processing Metrics: A Picture Story. ArXiv (2021)
14. Ristani, E., Solera, F., Zou, R.S., Cucchiara, R., Tomasi, C.: Performance Measures and a Data Set for Multi-Target, Multi-Camera Tracking. arXiv:1609.01775 [cs] (Sep 2016), <http://arxiv.org/abs/1609.01775>, arXiv: 1609.01775
 15. Russakovsky, O., Deng, J., Su, H., Krause, J., Satheesh, S., Ma, S., Huang, Z., Karpathy, A., Khosla, A., Bernstein, M., Berg, A.C., Fei-Fei, L.: ImageNet Large Scale Visual Recognition Challenge. *International Journal of Computer Vision* **115**(3), 211–252 (Dec 2015). <https://doi.org/10.1007/s11263-015-0816-y>, <https://doi.org/10.1007/s11263-015-0816-y>
 16. Sarlin, P.E., DeTone, D., Malisiewicz, T., Rabinovich, A.: SuperGlue: Learning Feature Matching with Graph Neural Networks. arXiv:1911.11763 [cs] (Mar 2020), <http://arxiv.org/abs/1911.11763>, arXiv: 1911.11763
 17. Sharan, L., Romano, G., Brand, J., Kelm, H., Karck, M., De Simone, R., Engelhardt, S.: Point detection through multi-instance deep heatmap regression for sutures in endoscopy. *International Journal of Computer Assisted Radiology and Surgery* **16**(12), 2107–2117 (Dec 2021). <https://doi.org/10.1007/s11548-021-02523-w>, <https://doi.org/10.1007/s11548-021-02523-w>
 18. Silverstein, E., Snyder, M.: Comparative analysis of respiratory motion tracking using Microsoft Kinect v2 sensor. *Journal of Applied Clinical Medical Physics* **19**(3), 193–204 (Mar 2018). <https://doi.org/10.1002/acm2.12318>, <https://www.ncbi.nlm.nih.gov/pmc/articles/PMC5978561/>
 19. Stern, A., Sharan, L., Romano, G., Koehler, S., Karck, M., De Simone, R., Wolf, I., Engelhardt, S.: Heatmap-based 2d landmark detection with a varying number of landmarks. In: Palm, C., Deserno, T.M., Handels, H., Maier, A., Maier-Hein, K.H., Tolxdorff, T. (eds.) *Bildverarbeitung für die Medizin 2021 - Proceedings, German Workshop on Medical Image Computing*, Regensburg, March 7-9, 2021. pp. 22–27. Informatik Aktuell, Springer (2021). https://doi.org/https://doi.org/10.1007/978-3-658-33198-6_7